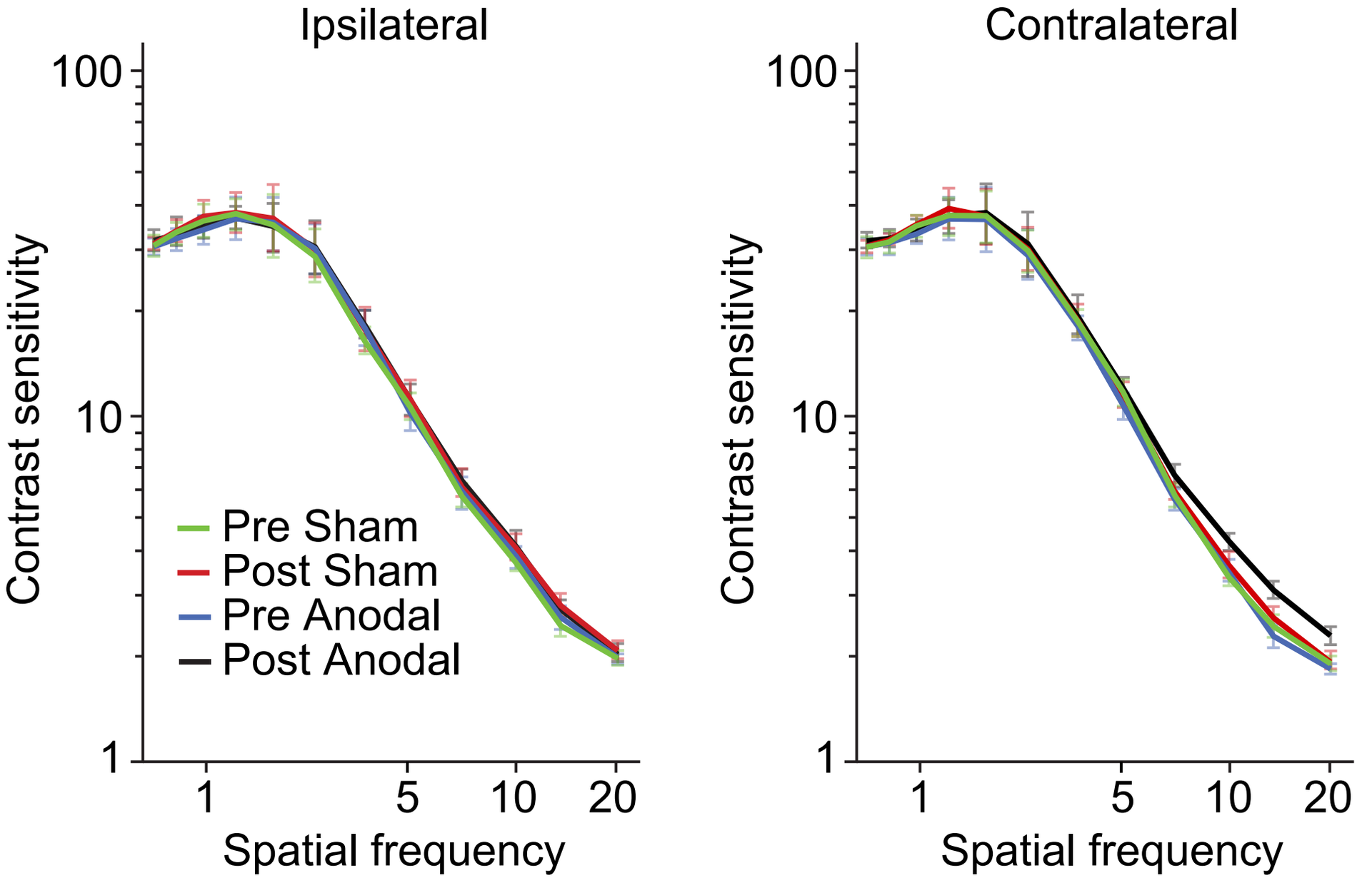
Ipsilateral
Contralateral
Contrast sensitivity
100
10
1
1
5
10
20
Spatial frequency
Pre Sham
Post Sham
Pre Anodal
Post Anodal

Figure S1

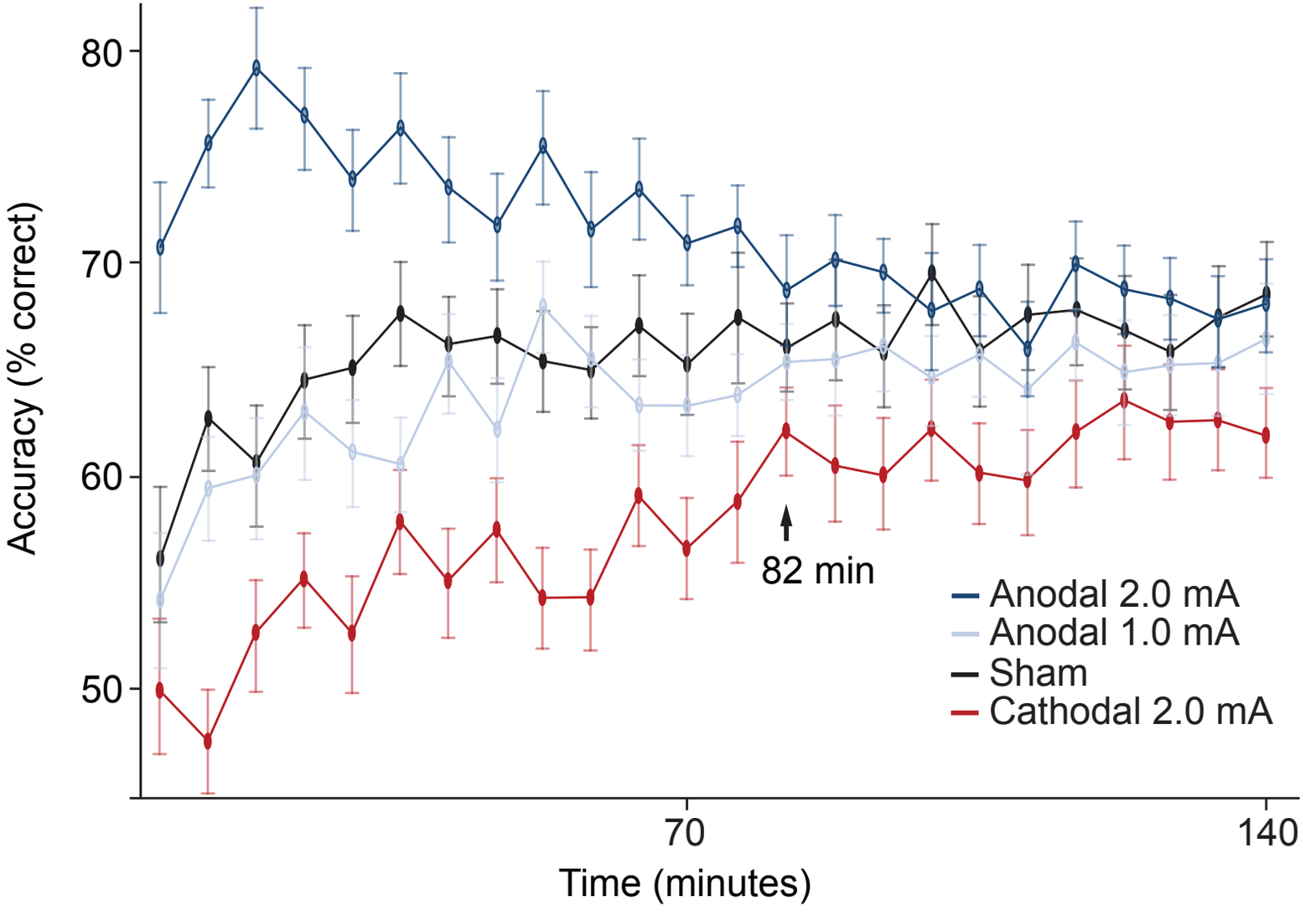
80
70
60
50
Accuracy (% correct)
82 min
Anodal 2.0 mA
Anodal 1.0 mA
Sham
Cathodal 2.0 mA
70
140
Time (minutes)

Figure S2

Supplemental Figure Legends

Figure S1. Results from Experiment 5. Contrast sensitivity as a function of spatial frequency (cycles per degree) before (Pre) and after (Post) the sham and anodal visual cortex tDCS. The data are sorted based on trials in which stimuli appeared in the ipsilateral (left panel) or contralateral (right panel) visual hemifields with respect to the location of stimulation. Error bars are ± 1 standard error of the mean. Figure S1 is related to the Experimental Design and the Supplemental Experimental Design.

Figure S2. Duration of transcranial direct-current stimulation effects during the vernier acuity task from Experiments 1-2. Mean performance accuracy (in percent correct) for stimuli appearing contralateral to tDCS application, collapsed across levels of vernier offset (2.2', 4.4', 6.6'), and sorted into 48-trial wide bins over the full 140-minute (or 2.3-hour) recording session from Experiments 1-2. Results from the 2.0 mA anodal (dark blue), 1.0 mA anodal (pale blue), sham (black), and 2.0 mA cathodal (red) conditions are shown based on the tDCS montage targeting visual cortex. The arrow marks the time interval (82 minutes from the start of the task) in which the stimulation conditions appear to converge. Error bars are ± 1 standard error of the mean. Figure S2 is related to the Discussion and the Supplemental Results and Discussion.

Table S1. Statistical results from Experiments 1, 2, 4, and 5.

Experiment 1	
	main effects of intensity
	2.0 vs. 1.5 vs. 1 mA, contralateral
RT	$F(2,38) = 4.645$, $d = 0.69$, $p = 0.016$
accuracy	$F(2,38) = 3.373$, $d = 0.59$, $p = 0.046$
	2.0 vs. 1.0 mA, contralateral
RT	$F(1,19) = 7.877$, $d = 0.91$, $p = 0.011$
accuracy	$F(1,19) = 4.570$, $d = 0.69$, $p = 0.046$
	2.0 vs 1.5 mA, contralateral
RT	$F(1,19) = 5.861$, $d = 0.78$, $p = 0.026$
accuracy	$F(1,19) = 4.945$, $d = 0.72$, $p = 0.038$
	2.0 vs. 1.5 vs. 1 mA, ipsilateral
RT	$F(2,38) = 0.425$, $d = 0.21$, $p = 0.647$
accuracy	$F(2,38) = 0.079$, $d = 0.09$, $p = 0.917$
	stimulation x location x intensity interactions
	contralateral
RT	$F(2,18) = 0.066$, $d = 0.08$, $p = 0.932$
accuracy	$F(2,18) = 0.233$, $d = 0.15$, $p = 0.793$
	ipsilateral
RT	$F(2,18) = 1.489$, $d = 0.30$, $p = 0.253$
accuracy	$F(2,18) = 0.048$, $d = 0.06$, $p = 0.950$
	main effects of intensity
	2.0 vs. 1.5 vs. 1 mA, contralateral
P1 amplitude	$F(2,38) = 3.400$, $d = 0.59$, $p = 0.053$
N1 amplitude	$F(2,38) = 6.295$, $d = 0.81$, $p = 0.010$
	2.0 vs. 1.0 mA, contralateral
P1 amplitude	$F(1,19) = 4.731$, $d = 0.70$, $p = 0.042$
N1 amplitude	$F(1,19) = 6.945$, $d = 0.85$, $p = 0.016$
	1.5 vs 1.0 mA, contralateral
P1 amplitude	$F(1,19) = 1.579$, $d = 0.40$, $p = 0.224$
N1 amplitude	$F(1,19) = 0.092$, $d = 0.09$, $p = 0.765$
	2.0 vs. 1.5 vs. 1 mA, ipsilateral
P1 amplitude	$F(2,38) = 0.479$, $d = 0.22$, $p = 0.619$
N1 amplitude	$F(2,38) = 0.087$, $d = 0.09$, $p = 0.901$
	1.5 vs 1.0 mA, ipsilateral
P1 amplitude	$F(1,19) = 0.469$, $d = 0.22$, $p = 0.502$
N1 amplitude	$F(1,19) = 0.012$, $d = 0.03$, $p = 0.913$
Experiment 2	
	main effects of stimulation
RT	2.0 mA vs. sham, contralateral
accuracy	$F(1,19) = 5.502$, $d = 0.76$, $p = 0.030$
	2.0 mA vs. sham, ipsilateral
RT	$F(1,19) = 0.003$, $d = 0.01$, $p = 0.956$
accuracy	$F(1,19) = 0.517$, $d = 0.23$, $p = 0.481$

	2.0 mA vs. sham, contralateral
P1 amplitude	$F(1,19) = 1.494$, $d = 0.39$, $p = 0.236$
N1 amplitude	$F(1,19) = 5.367$, $d = 0.75$, $p = 0.032$
	2.0 mA vs. sham, ipsilateral
P1 amplitude	$F(1,19) = 0.017$, $d = 0.04$, $p = 0.897$
N1 amplitude	$F(1,19) = 0.025$, $d = 0.05$, $p = 0.877$
Experiment 4	
	main effect of time
	pre vs. post, anodal
logMAR	$F(1,19) = 11.862$, $d = 1.11$, $p = 0.003$
	pre vs. post, sham
logMAR	$F(1,19) = 3.788$, $d = 0.63$, $p = 0.067$
	stimulation x time interaction
logMAR	$F(1,19) = 4.500$, $d = 0.68$, $p = 0.047$
	subject-wise correlation
logMAR	$r(1,19) = -0.603$, $p = 0.005$
Experiment 5	
	stimulation x time interaction
	contralateral
contrast sensitivity	$F(1,19) = 16.003$, $d = 1.29$, p = 0.001
	ipsilateral
contrast sensitivity	$F(1,19) = 0.205$, $d = 0.14$, $p = 0.656$
	Main effect of time
	anodal, contralateral
contrast sensitivity	$F(1,19) = 16.316$, $d = 1.31$, $p = 0.001$
	sham, contralateral
contrast sensitivity	$F(1,19) = 0.351$, $d = 0.19$, $p = 0.561$
	anodal, ipsilateral
contrast sensitivity	$F(1,19) = 0.538$, $d = 0.23$, $p = 0.472$
	sham, ipsilateral
contrast sensitivity	$F(1,19) = 0.525$, $d = 0.23$, $p = 0.477$
	Time x frequency interaction
	anodal, contralateral
contrast sensitivity	$F(11,209) = 3.290$, $d = 0.58$, $p = 0.013$
	sham, contralateral
contrast	$F(11,209) = 0.107$, $d = 0.10$, $p = 0.763$

sensitivity	
	anodal, ipsilateral
contrast sensitivity	$F(11,209) = 1.145$, $d = 0.34$, $p = 0.321$
	sham, ipsilateral
contrast sensitivity	$F(11,209) = 0.296$, $d = 0.17$, $p = 0.685$
	main effect of time
	anodal, contralateral
	frequency 0.50
contrast sensitivity	$F(1,19) = 2.178$, $d = 0.47$, $p = 0.156$
	frequency 0.69
contrast sensitivity	$F(1,19) = 0.064$, $d = 0.08$, $p = 0.804$
	frequency 0.97
contrast sensitivity	$F(1,19) = 0.192$, $d = 0.14$, $p = 0.666$
	frequency 1.36
contrast sensitivity	$F(1,19) = 0.087$, $d = 0.09$, $p = 0.772$
	frequency 1.91
contrast sensitivity	$F(1,19) = 2.879$, $d = 0.55$, $p = 0.106$
	frequency 2.67
contrast sensitivity	$F(1,19) = 2.527$, $d = 0.51$, $p = 0.128$
	frequency 3.73
contrast sensitivity	$F(1,19) = 1.926$, $d = 0.45$, $p = 0.181$
	frequency 5.22
contrast sensitivity	$F(1,19) = 1.722$, $d = 0.42$, $p = 0.205$
	frequency 7.31
contrast sensitivity	$F(1,19) = 5.623$, $d = 0.76$, $p = 0.028$
	frequency 10.22
contrast sensitivity	$F(1,19) = 10.556$, $d = 1.05$, $p = 0.004$
	frequency 14.30
contrast sensitivity	$F(1,19) = 9.517$, $d = 1.00$, $p = 0.006$
	frequency 20.00
contrast sensitivity	$F(1,19) = 13.252$, $d = 1.18$, $p = 0.002$

Supplemental Experimental Procedures

Subjects

There were 100 different subjects who participated across five experiments (Experiment 1, N = 20, 11 women, mean age ± SEM, 22.0 ± 0.9; Experiment 2, N = 20, 7 women, 25.3 ± 1.3; Experiment 3, N = 20, 13 women, 23.1 ± 1.2; Experiment 4, N = 20, 10 women, 22.4 ± 1.3; Experiment 5, N = 20, 6 women, 20.4 ± 1.8). All subjects self reported having normal color vision and normal or corrected-to-normal visual acuity. Subjects gave informed written consent to procedures approved by the Vanderbilt University Institutional Review Board and were compensated at a rate of $10 per hour for their time. We had 6 subjects voluntarily withdraw from Experiment 1, and 3 subjects from Experiment 3. In addition, 2 subjects from Experiment 1, and 1 subject from Experiment 2 were removed due to excessive eye movements (eye movement measurement and rejection criteria are described below).

Stimuli and Procedure

Vernier Acuity Task. The vernier acuity task was in Experiments 1-3. An example of the sequence of events on each trial is shown in **Figure 1B**. The fixation point was presented for 1000 ms prior to the onset of the vernier stimuli. The vernier stimuli were then presented for 54 ms. Immediately after the offset of the venier stimuli, a random visual noise mask was presented for 200 ms. Subjects pressed one of two buttons on a handheld gamepad to indicate whether the top line was to the right or left of the bottom line. Trial-by-trial feedback was presented for 1000ms following the registration of each response. The inter-trial interval was 1000-1200 ms, randomly jittered with a rectangular distribution. Vernier acuity is also known as hyperacuity because resolution at the fovea is less than the width of the dendritic tree of a photoreceptor [S1-S3]. We randomly varied the displacement of the two lines between 2.2, 4.4, and 6.6 arc minutes of gap offset, with the two line segments centered 5° of visual angle in the left or right visual field.

Stimuli were viewed on a gray background (54.3 cd/m^2) from a distance of 85 cm. A black fixation cross (<0.01 cd/m^2, 0.4° x 0.4° of visual angle) was visible throughout each trial. The vernier stimuli were two vertical line segments. One vertical line was presented above the other. Each of the two vertical line segments subtended 0.44° height x 0.1° width of visual angle, centered 5° in the periphery (i.e., a location in the parafoveal belt) [S4]. The two lines were separated by a vertical gap of 8.8', and the upper line was displaced 2.2', 4.4', or 6.6' to the left or right of the lower line.

The vernier stimuli appeared to the left of fixation on half of the trials and to the right on the remainder, with the two types randomly interleaved across trials. Across all trials, the three gap offsets were randomly sampled with equal probability (33.3%), and the displacement to the left or right of the lower line was also equiprobable (50%). The visual noise mask was a 1.4° x 1.4° square. The mask was centered on the location of the vernier stimuli. The visual noise mask was generated by randomly selecting the luminance of each cell of a 130 x 130 matrix with replacement.

Subjects were instructed to press one button using a handheld gamepad if the upper line was displaced to the left of the lower line, and a second button if the upper line was displaced to the right of the lower line. The duration, eccentricity, and masking of the vernier stimuli allowed us to avoid ceiling effects and keep overall performance at approximately 70%, consistent with previous work [S5]. The trial-by-trial feedback was a centrally presented outline of a circle (0.88° diameter, 0.13° thick) or cross (0.88° length, 0.13° thick), presented for 1000 ms immediately following each response, with the meaning of these symbols (i.e., correct versus incorrect) randomized across days and subjects. Each subject was given 96 practice trials. The task consisted of 1,152 trials with 30-second breaks every 100 trials.

Snellen Acuity Task. The Snellen acuity task was used in Experiment 4. We chose to use the Snellen chart so that we could generalize our findings from the vernier acuity task to a standard measure of visual acuity used outside the laboratory. The chart has letters of different sizes arranged from largest at the top to smallest at the bottom. Subjects read through the chart using one eye at a time. Subjects viewed the letters from a distance of 6 meters (or 20 feet). Based on this viewing distance and the reference standard (known today as 20/20), the 8^{th} row of letters from the top of the chart consisted of letters subtending an angle of 5° with each letter part subtending 1°. Subjects started at the top of the chart and read each letter aloud to an experimenter who scored their performance. The Snellen exam was

conducted in a quiet, well-illuminated room with a full 20-foot lane (i.e., no mirrors necessary). Eleven subjects had corrected-to-normal visual acuity and used contacts or eyeglasses during the Snellen task. Two subjects who self reported having correct-to-normal visual acuity had Snellen acuity slightly below 20/20. However, when we reran all analyses with these two low-acuity subjects removed from the sample, all results remained significant, including the acuity improvement observed between pre versus post time points in the anodal condition (main effect of time on logMAR score $F_{(1, 17)} = 16.347$, $d = 1.31$, $p = 0.001$), the time (pre versus post) x condition (sham versus anodal) interaction ($F_{(1, 17)} = 4.991$, $d = 0.72$, $p = 0.039$), and the subject-wise correlation between Snellen acuity at baseline and the stimulation-induced improvement in Snellen acuity ($r_{(1,17)} = -0.493$, $p = 0.038$).

Contrast sensitivity. In Experiment 5, we investigated the effects of the visual cortex stimulation on contrast perception by examining subjects' contrast sensitivity function (CSF). We implemented the quick CSF (qCSF) method, which provides an assessment of the complete shape of the CSF using a Bayesian adaptive simulation procedure [S6]. The rapid measurement of CSF allowed us to avoid bias in the results related to fatigue given the time-consuming nature of traditional CSF measurement, and obtain data immediately after electrical stimulation during which the impact of the stimulation was found to be strongest (see **Figure S1** and see **Table S1** for the results of the statistical analyses of Experiment 5).

Experiment 5 used a two interval forced choice target detection task. We changed the display on a 13-inch color CRT monitor (65-Hz refresh rate) to monochromatic, with 10-bit gray scale resolution, and linearized luminance values via a lookup table [S7]. Stimuli were Gaussian-windowed sinusoidal gratings, oriented ± 45° from vertical, randomly interleaved across trials to the left or right of central fixation (5° eccentricity), rendered on a 400 x 400 pixel grid, subtending 5.6° x 5.6°, and viewed binocularly at roughly 80.5 cm in dim light. There were 12 possible grating spatial frequencies spaced log linearly from 0.5 to 20 cycles per degree (cpd), and 60 possible grating contrasts spaced log linearly from 0.1 to 100%. The stimulus sequence started with the presentation of a central fixation cross (500 ms), followed by a target-grating stimulus (130 ms). The target coincided with one of two consecutive auditory tones (500 and 1000 Hz, 130 ms). The auditory tones informed subjects of the two possible time intervals in which a grating target could appear and reduced stimulus uncertainty, which has been shown to affect CSF measurement, especially in the high-frequency region [S8]. Subjects pressed one button if they detected the target in the first interval, and a second button if they detected the target in the second interval.

The qCSF method uses the truncated log-parabola to characterize the CSF with four parameters (i.e., peak sensitivity or gain, peak spatial frequency, bandwidth in octaves, and low-frequency sensitivity truncation level) [S6]. A four dimensional probability density function is used to assign probabilities for combinations of the parameters. The spatial frequency and contrast of the stimulus on each trial is determined by the probability density function, which is updated with Bayes rule based on the subjects' response from the previous trial. From each qCSF measurement, the expectation value of the contrast sensitivity at individual spatial frequencies was estimated from the four-dimensional probability density function that was obtained at the end of 100 trials in each qCSF measurement, as described by Lesmes et al. (2010). This procedure calculates the most probable contrast sensitivity value for each spatial frequency. The individual contrast sensitivity values for 12 spatial frequencies between 0.5 and 20 cpd were analyzed.

Experimental Design

All experiments began with 20 minutes of transcranial direct-current stimulation (tDCS) applied over visual cortex (Experiments 1, 2, 4, and 5) or motor cortex (Experiment 3). Immediately following, subjects performed the vernier acuity task (Experiments 1-3), Snellen acuity task (Experiment 4), or contrast sensitivity task (Experiment 5) while we measured their behavior (Experiments 1-5) and electrical brain activity (Experiments 1-2). All experiments had a within-subjects design. That is, each subject completed all of the stimulation conditions to remove individual differences being confounded with the effects of stimulation.

In Experiment 1, we stimulated visual cortex with anodal tDCS and examined the effects of the stimulation on the electrophysiology and behavior during the vernier acuity task. We varied stimulation intensity across three levels (1.0 mA, 1.5 mA, and 2.0 mA anodal) administered across three separate testing days, with order randomized for each subject. Our goal was to determine the stimulation intensity that resulted in the maximum improvement in behavioral performance. After establishing that 2.0 mA of stimulation was maximally effective, we focused on this stimulation intensity and compared it with the sham control conditions in subsequent experiments.

In Experiment 2, we stimulated visual cortex with cathodal tDCS and examined the effects of stimulation on the electrophysiology and behavior during the vernier acuity task. Two different stimulation conditions (2.0 mA cathodal and a sham baseline) were administered across two separate testing days, order counterbalanced across subjects. In Experiment 3, we stimulated motor cortex with anodal tDCS and examined the effects of stimulation on behavioral metrics from the vernier acuity task. Two different stimulation conditions (2.0 mA anodal and sham baseline) were administered across two separate testing days, order counterbalanced across subjects. In Experiment 4, we stimulated visual cortex with anodal tDCS and examined the effects of stimulation on the Snellen acuity task. Snellen acuity scores were collected before and after the 2.0 mA anodal stimulation on one day, and before and after the baseline sham stimulation on another day. In Experiment 5, we stimulated visual cortex with anodal tDCS and examined the effects of stimulation on contrast perception. Contrast sensitivity function values were collected before and after the 2.0 mA anodal stimulation on one day, and before and after the baseline sham stimulation on another day, order counterbalanced across subjects. All experiments counterbalanced the hemisphere being stimulated across subjects, and tested for effects of hemisphere, although none were found, indicating symmetry of the stimulation effects across hemispheres. In all experiments, testing immediately followed the electrical stimulation.

Transcranial Direct-Current Stimulation

Apparatus and Procedure. The tDCS was administered using a battery driven, constant current stimulator (Mind Alive Inc., Alberta, Canada) and pair of conductive rubber electrodes (active: 19.25 cm^2 reference: 52 cm^2). The electrodes were placed in saline-soaked sponges and held in place by a headband. Current was applied for 20 min over the left and right hemispheres (counterbalanced across subjects) of visual cortex (site P1 and P2 of the International 10-20 System) in Experiments 1, 2, 4, and 5, and over the left and right hemispheres (counterbalanced across subjects) of motor cortex (site C3 and C4) in Experiment 3. In Experiments 1, 3, 4, and 5 the anodal electrode on the head was paired with a cathodal electrode centered over the ipsilateral cheek to avoid confounding effects from other brain regions [S9, S10]. The direction of current was reversed in Experiment 2, such that the cathodal electrode was located on the head and the anodal electrode was over the ipsilateral cheek. Specifically, the cheek electrode was placed diagonally, 3 cm from the cheilion (lip corner at rest) along an imaginary line connecting the cheilion to the ipsilateral condylion (palpable when the jaw is moved) (**Figure 1A**).

Stimulation intensity varied across three levels (1.0 mA, 1.5 mA, and 2.0 mA) in Experiment 1, and was fixed at 2.0 mA in Experiments 2-5. Comparable stimulation protocols have been shown to cause effects lasting from 90 min [S11] up to 5 hr [S10]. The time interval between testing days was greater than 48 hours to minimize potential carryover effects related to repeated brain stimulation exposure [S12]. In Experiments 2-5, the sham tDCS condition followed the same procedure as the active tDCS, but stimulation only lasted 30 seconds, ramping up and down at the beginning and end of the 20-minute period. This sham procedure results in the same tingling and itching sensations associated with active tDCS. All subjects confirmed experiencing a mild tingling or itching sensation during the sham condition, and subjects were unable to distinguish between sham and active stimulation, as we discuss next.

We took two measures to ensure that subjects' expectations about the experimental procedures did not bias the results. First, subjects were blind to the intensity (Experiment 1) or presence (Experiments 2-5) of stimulation. Blinding was confirmed through a series of debriefing questions. Specifically, after each testing day, subjects completed a safety questionnaire [S13] and visual analog scale [S14], which included questions regarding attention, concentration, mood, vision, headache, fatigue, and skin sensations under the tDCS electrodes. We found that the scores from these ratings did not significantly differ between stimulation conditions in Experiments 1-5 ($Fs < 1.243$, $ps > 0.280$). In addition, after the final day of testing, all subjects were directly asked to guess on which testing days they had received the various stimulation intensities (Experiment 1) or active versus sham stimulation (Experiments 2-5). Overall, subjects were near chance at detecting the proper intensity (33%) or presence (50%) of stimulation (Experiment 1: hit rate 25%; Experiment 2: hit rate 45%, Experiment 3: hit rate 55%; Experiment 4: hit rate 55%; Experiment 5: hit rate 50%). When we sorted the subjects based on those who guessed correctly versus incorrectly on this debriefing question, we found the same pattern of results for both groups across all of the experiments, and no significant differences as a function of response group. Second, to rule out potential confounding factors related to the order in which stimulation was presented, we examined whether stimulation order was introducing bias on our dependent variables. We found no interaction between stimulation order and the factors used in our statistical tests, including stimulation (i.e., active versus sham), stimulation intensity, stimulation location, target laterality, difficulty level, or time on any of our measures from Experiment 1 ($Fs < 1.1203$, $ps > 0.325$), Experiment 2 ($Fs < 2.045$, $ps >$

0.111), Experiment 3 ($Fs < 1.702$, $ps > 0.200$), Experiment 4 ($Fs < 0.468$, $ps > 0.582$), or Experiment 5 ($Fs < 2.214$, $ps > 0.171$) verifying the effectiveness of the order randomization method we used across subjects.

Current-flow Modeling. To maximize stimulation of the targeted regions, tDCS electrode montages were configured and optimized based on current-flow modeling (HD-Target, HD-Explore, Soterix Medical, NY) and previous research methods [S15]. Current-flow models used a finite element method to compute the distribution of the electric field into a standard adult head model. The modeling results shown in **Figures 1A**, **2A**, and **3A** show the estimated electric field orientation and intensity in targeted areas, based on the selected montages. As with our previous modeling work [S10, S15-S17], we do not regard these estimates as definitive solutions about the exact location of current flow during stimulation. However, these models do serve as working hypotheses for how the current flow is spatially distributed through the brain, and offer potential target locations for investigators using techniques in human neuroimaging or animal neurophysiology.

Electrophysiology

For Experiments 1-3, the testing was conducted in a double-walled sound-attenuating electrically shielded isolation booth to eliminate external sources of electrical noise. For Experiments 1 and 2, the raw electroencephalogram (EEG) was recorded (250 Hz sampling rate, 0.01 to 100-Hz bandpass filter) with an SA Instrumentation amplifier using non-polarizable tin electrodes embedded in an elastic cap (Electrocap International, Eaton, OH). The recording electrodes were arrayed according to the International 10/20 System (Fz, Cz, Pz, F3/F4, C3/C4, P3/P4, PO3/PO4, T3/T4, T5/T6, O1/O2) including 2 nonstandard sites (OL, midway between O1 and T5; and OR, midway between O2 and T6). Signals were referenced online to the right mastoid electrode and re-referenced offline to the average of the left and the right mastoids [S18]. Horizontal eye position was monitored by recording electrooculogram (EOG) from bipolar electrodes placed at the outer canthi of each eye. Vertical eye position and blinks were monitored with bipolar electrodes placed above and below the left eye. Peri-orbital electrodes detected eye movements and a two-step ocular artifact rejection method was used [S19], resulting in the removal of 2 subjects from Experiment 1, and 1 subject from Experiment 2 for excessive eye movements (either > 25% of individual trials rejected or any residual systematic eye movement that resulted in HEOG voltage deflections > 3.2 μV, corresponding to an ocular deviation of ± 0.1°).

Data Analysis

Event-related Potentials. To confirm that tDCS was changing how the visual system was processing information early in the processing stream, we recorded the early event-related potential (ERP) components known to index sensory and perceptual processing [S20]. The EEG was time-locked to the onset of the vernier stimuli, baseline corrected to the period from -200 to 0 ms prior to stimulus onset, and displayed from -100 to 250 ms relative to stimulus onset. The P1 and N1 components were measured from lateral occipital electrodes (OL/R) where these components are maximal. We quantified mean amplitude using 50-ms long measurement windows centered on the peak of the P1 and N1 waveforms (P1: 75 to 125 ms; N1: 140 to 190 ms) [S20]. Grand average waveforms were 35 Hz low-pass filtered for presentation purposes, but all analyses were performed on unfiltered waveforms. Voltage topographies were calculated using spherical-spline interpolation [S21].

Snellen Acuity. Our measure of Snellen acuity was calculated using the letter assignment scoring method where subjects earned credit for correctly naming individual letters on the Snellen chart, as opposed to line assignment method which requires correctly reading a complete line of the letters. Letter-based scoring allowed us to overcome several disadvantages of Snellen charts. For example, letter-based scoring allows measurement of visual acuity on a finer scale. In contrast, by using line assignment with variable letters per line, a change in acuity of one letter can yield a change of vision of an entire line. Second, because of the lack of standardized progression between lines, Snellen acuity is difficult to examine statistically using line-based scoring. To remedy this, we obtained letter-based scores and converted them to the standard geometric notation for expressing visual acuity, called the logarithm of the minimal angle of resolution (LogMAR). LogMAR is the logarithm to the base 10 of the angular subtense of the stroke widths at 6 meters (or 20 feet). The minimal angle of resolution (or MAR) is the width of one bar on a Snellen E. In logMAR notation, lower scores denote better acuity, and vision becomes worse as the logMAR values increases. A logMAR of 0 is equivalent to 20/20 vision.

In addition to choosing a more rigorous scoring method, we made efforts to minimize the underlying variability in the Snellen chart measurement. To do this, our Snellen acuity experiment was a within-subjects design, and consisted of pre- and post-stimulation Snellen testing on both the active tDCS day and the sham tDCS day. This allowed us to capture the test-retest variability on each day and reduce spurious statistical results when calculating the effects of stimulation on Snellen acuity. It is important to note that the Snellen test is common in clinical practice, not vision research. Our primary reason for using the Snellen chart was not because of its scientific merits as a rigorous experimental assessment, but rather, because the Snellen chart is widely used among clinicians to measure visual acuity, and thus provides the opportunity to test the real-world applicability of the visual cortex stimulation protocol that we used in this study. Moreover, despite its shortcomings, the measurement of Snellen acuity has provided a critical data point for comparison with other systematic measurements of visual field function in basic and clinical research [S22-S31].

Statistical Analysis. Across the five experiments, we computed analyses of variance (ANOVAs) using the within-subjects factors of stimulation (anodal vs. sham or cathodal vs. sham), stimulation intensity (1.0 mA vs. 1.5 mA vs. 2.0 mA), stimulation location (left hemisphere vs. right hemisphere), stimulus laterality (contralateral vs. ipsilateral), vernier offset difficulty (2.2', 4.4', 6.6'), and time (pre stimulation vs. post stimulation) on our dependent measures, including RT, accuracy, logMAR score, contrast sensitivity, and the amplitudes of P1 and N1 components. Trials were binned according to the location of vernier stimuli with respect to the hemisphere that had been electrically stimulated (i.e., ipsilateral or contralateral). Also, trials were binned according to the level of the task difficulty determined by the gap-offset distance between vernier stimuli (i.e., 2.2', 4.4', or 6.6'). Where appropriate, follow up ANOVAs were conducted to test specific preplanned hypotheses. P-values were adjusted using the Greenhouse-Geisser epsilon correction for nonsphericity when this assumption was violated [S32]. Finally, we calculated Cohen's d effect size estimates [S33] for each analysis to facilitate comparisons between studies and promote replication.

Supplemental Results and Discussion

We found that tDCS over visual cortex modulated vernier acuity for well over 1 hour. **Figure S2** shows the within-session dynamics of mean accuracy in the vernier acuity task from Experiments 1-2. These data were obtained from trials in which stimuli appeared contralateral to tDCS application, collapsed across the difficulty levels of vernier offset (i.e., 2.2', 4.4', 6.6'), and sorted into 48-trial wide bins across the full 2.3-hour recording session. We calculated two-tailed t-tests at each time bin between stimulation conditions. To determine when the tDCS effects wore off, we searched the behavioral time series for time bins where there were no significant ($p > 0.05$) between-condition differences, provided they were followed by at least 5 consecutive non-significant time bins (i.e., roughly 30 minutes of task) to ensure the stability of performance over time.

For the anodal tDCS of Experiment 1, we found that relative to the 1.0 mA intensity, accuracy improvements following 2.0 mA stimulation were largest during the first hour of the task, but that these advantages in vernier acuity were no longer statistical significant after approximately 82 minutes. A similar result was found when comparing the 2.0 mA anodal condition of Experiment 1 to the baseline sham condition of Experiment 2. In addition, the behavioral dynamics following the 2.0 mA cathodal tDCS also converged with the baseline sham condition after approximately 82 minutes from the start of the task. However, after this 82-minute period, we observed changes in behavior that significantly differed from baseline, suggesting that subjects may not have fully recovered from the cathodal stimulation effects by the end of the experiment. It seems likely that these long lasting after effects of tDCS may still be influencing behavior at the end of our recordings, and that significantly longer follow-up experiments will be needed to observe when the benefits of anodal tDCS and the costs of cathodal tDCS truly disappear. Importantly, these results demonstrate that a single dose of 20 minutes of anodal tDCS over visual cortex is powerful enough to produce spatial resolution benefits in the parafoveal belt (i.e., 5° eccentricity) lasting well over 1 hour in healthy young adults with normal vision, highlighting the translational potential of the brain stimulation protocol we have developed. This is striking given that previous studies using tDCS of primary visual cortex [S34-S38] have tended show mostly online effects (i.e., during stimulation) with relatively transient offline effects (i.e., < 10 min following stimulation), including those for contrast sensitivity [S34], motion detection thresholds [S39] and perception of phosphenes [S37, S38]. In contrast, our results show far more enduring and lasting effects of visual perception offline. In addition, it is possible that the duration of the stimulation results on visual acuity may be greater for individuals with poorer vision, given our findings from Experiment 4 using the Snellen chart, and that repeated stimulation combined with behavioral training could offer more lasting benefits.

The duration findings allow us to address the possibility that occipitoparietal tDCS defocused subjects' vision during the 20-minute period of stimulation, resulting in a neural compensation and visual improvement, similar to enhancements in vision following time without refractive correction [40]. Defocus induced blur adaption has been reported to modify supra-threshold contrast sensitivity at multiple spatial frequencies, from 3.22 [S41], 8, 12 [S42], up to 25 cpd [S40], and for stimuli presented at the fovea and locations of the parafoveal nasal visual field (2°, 4°, 6°, 8°, 10°) with best-corrected distance vision [S43]. Adaptation changes in contrast sensitivity can influence letter acuity, and studies have found that changes in high contrast letter acuity following defocus adaptation ranges from two letters when adjusting to subjects' own myopic refractive error [S44] to approximately three lines while adapting to +2.50 D blur [S45]. Critically, the majority of these effects are observed online, and when aftereffects are examined they typically last approximately 5 minutes [S41]. By contrast, in the present study we found offline effects with significantly longer lasting improvements in vision. These data argue against the view that the tDCS-triggered improvements were due to defocus induced blur adaptation. Nonetheless, we believe this question requires future work with more definitive assessment techniques.

The results from Experiments 1 and 2 allow us to rule out several alternative explanations for the effects we observed. It is possible that the direct-current stimulation changed the deployment of visual-spatial attention, such that the focus of attention was biased toward the visual field contralateral to the stimulation [S46, S47]. However, if tDCS had biased attention in this way, then we should have observed the opposite pattern of effects ipsilateral to the stimulation, because capacity limits define mechanisms of attentional selection [S48]. For example, if tDCS worked like a spatial cue, resulting in a shift of visual-spatial attention into the left visual hemifield, then this benefit should improve processing for left visual field stimuli at the expense of processing right visual field stimuli. Contrary to this prediction, our results consistently showed effects contralateral to the tDCS, with no accompanying tradeoff for ipsilaterally presented stimuli. Previous work with the vernier task indicates that the absence of task-irrelevant distractors and the use of just two spatial locations for the vernier stimuli make it unlikely that attention would play a significant role in this task [S49, S50]. The next explanation that we can rule out is that tDCS changed the precision of spatial vision by altering pupil dilation and accommodation [S51]. However, if this had been the case, then we would not have observed effects in one hemifield but not the other. Thus, the present results and paradigm provide evidence that tDCS changed sensory-level activity in the cortex leading to a systematic modulation of the precision of spatial vision and are difficult to account for with alternative explanations based on attention, pupil dilation, or accommodation.

The electrophysiological evidence from Experiments 1-2 suggest the occipitoparietal tDCS induced changes in vernier acuity by augmenting early stages of neural information processing. In the main text, we focus on the two canonical visual evoked potentials (i.e., the P1 and N1) hypothesized to derive from extrastriate visual areas [20]. Here, we assess an even earlier component called the C1, which is typically observed between 65 and 90 ms poststimulus onset and thought to have neural generators in primary visual cortex [52-54]. We found no significant effects of anodal stimulation intensity on C1 amplitude in Experiment 1 (contralateral, $F_{(2, 38)} = 1.961$, $d = 0.45$, $p = 0.162$; ipsilateral, $F_{(2, 38)} = 0.297$, $d = 0.17$, $p = 0.714$), and no effect of cathodal stimulation on C1 amplitude in Experiment 2 (contralateral, $F_{(1, 19)} = 2.091$, $d = 0.46$, $p = 0.164$; ipsilateral, $F_{(1, 19)} = 1.316$, $d = 0.37$, $p = 0.266$). These results demonstrate the offline temporal specificity of the stimulation effects on the neural mechanisms of visual perceptual processing. The findings across Experiments 1-2 suggest that the behavioral changes we observed in visual acuity following occipitoparietal tDCS were due to the stimulation having changed an intermediate stage of processing likely involving regions of extrastriate visual cortex.

In Experiment 3 we wanted to determine if the improvements in spatial vision that we measured in Experiment 1 were specific to stimulation of visual cortex, or would be observed following any lateralized stimulation of the human brain. For example, perhaps the lateralized stimulation increases arousal of the subjects or results in subjects expecting to perform better contralateral to the stimulation (i.e., demand characteristics).

In Experiment 3 we stimulated motor cortex of subjects (left or right, counterbalanced across subjects) with 2.0 mA of anodal stimulation or sham (see **Figure 3A**). All subjects performed both conditions with order counterbalanced. We found that subjects simply responded with greater overall speed regardless of the visual field the stimuli (main effect of stimulation on RTs: $F_{(1, 19)} = 11.031$, $d = 1.07$, $p = 0.004$) (see **Figure 3B**). Further, unlike the spatially mapped pattern of performance observed after visual cortex tDCS, we observed behavioral RT advantages for stimuli presented in both hemifields (contralateral: $F_{(1, 19)} = 4.704$, $d = 0.70$, $p = 0.043$; ipsilateral: $F_{(1,}$

$_{19)}$ = 4.490, d = 0.68, p = 0.047) and no stimulation x target laterality interaction ($F_{(1, 19)}$ = 0.014, d = 0.03, p = 0.906). Third, there was no improvement in accuracy ($F_{(1, 19)}$ = 1.506, d = 0.39, p = 0.235) (see **Figure 3C**). If anything we observed a slight decline in accuracy across conditions, suggesting that motor cortex stimulation resulted in a speed-accuracy tradeoff. These results show that the improvements we observed previously were specific to tDCS of visual cortex.

The present study provides new information to a growing body of work focused on developing interventions for the remediation of visual deficits in patient populations. Studies using behavioral training have shown that practice can boost vernier acuity [S25, S55] contrast sensitivity, and letter recognition [S22] in adult amblyopia, with effects lasting for months [S22, S25, S30] to a year or more [S22, S28]. Similarly, action videogame training in amblyopia patients has been shown to result in a range of improved spatial and temporal visual functions including visual acuity [S56]. In addition to behavioral interventions, the use of non-invasive brain stimulation techniques for the treatment of vision disorders, such as amblyopia is rapidly developing [S57-S59], and tDCS is particularly attractive due to its low cost and portability. Specifically, tDCS in conjunction with training protocols offers advantages such as shortened training time, which without stimulation often requires thousands of trials over days to weeks of practice, as well as generating more potent and enduring perceptual improvements. For example, visual benefits in contrast sensitivity and uncorrected visual acuity (a gain of 0.15 logMAR) following 2 months of perceptual training can be reduced to only 2 weeks of training when coupled with noninvasive brain stimulation [S60]. Moreover, improvements in visual acuity and stereopsis in adults with amblyopia have been shown to be more pronounced and longer lasting following 2 weeks of anodal tDCS over primary visual cortex combined with videogame-based dichoptic perceptual training as compared with dichoptic training alone [S61]. Anodal tDCS of visual cortex coupled with behavioral training has also been reported to enhance the rehabilitation of visual field deficits after stroke [S62, S63]. The present findings raise the possibility for further capitalizing on the experience-dependent plasticity mediating performance- and stimulation-induced visual enhancements, and for optimizing interventions with the goal of speeding recovery following visual cortical damage and rescuing function in patients with vision disorders. In addition, the contrast sensitivity improvements measured in Experiment 5 with 50% contrast suggest that acuity benefits could be even larger than the 15% improvement we found here under 100% contrast with Vernier stimuli.

Supplemental References

S1. Baker, T.Y., and Bryan, G.B. (1912). Errors of observation. In Proceedings of the Optical Convention, H.a. Stroughton, ed. (London).

S2. Berry, R.N. (1948). Quantitative relations among vernier, real depth, and stereoscopic depth acuities. Journal of Experiment al Psychology *38*, 708-721.

S3. Westheimer, G., and McKee, S.P. (1977). Spatial configurations for visual hyperacuity. Vision Research *17*, 941-947.

S4. Schira, M.M., Tyler, C.W., Breakspear, M., and Spehar, B. (2009). The foveal confluence in human visual cortex. Journal of Neuroscience *29*, 9050-9058.

S5. Yeshurun, Y., and Carrasco, M. (1999). Spatial attention improves performance in spatial resolution tasks. Vision Research *39*, 293–305.

S6. Lesmes, L.A., Lu, Z.-L., Baek, J., and Albright, T.D. (2010). Bayesian adaptive estimation of the contrast sensitivity function: The quick CSF method. Journal of Vision *10*, 1-21.

S7. Li, X., Lu, Z.L., Xu, P., Jin, J., and Zhou, Y. (2003). Generating high gray-level resolution monochrome displays with conventional computer graphics cards and color monitors. Journal of Neuroscience Methods *130*, 9–18.

S8. Woods, R.L. (1996). Spatial frequency dependent observer bias in the measurement of contrast sensitivity. Ophthalmic and Physiological Optics *16*, 513–519.

S9. Tseng, P., Hsu, T.-Y., Chang, C.-F., Tzeng, O., Hung, D., Muggleton, N., Walsh, V., Liang, W.-K., Cheng, S.-k., and Juan, C.-H. (2012). Unleashing Potential: Transcranial direct current stimulation over the right posterior parietal cortex improves change detection in low-performing individuals. Journal of Neuroscience *32*, 10554-10561.

S10. Reinhart, R.M.G., and Woodman, G.F. (2014). Causal control of medial-frontal cortex governs electrophysiological and behavioral indices of performance monitoring and learning. Journal of Neuroscience *34*, 4214-4227.

S11. Nitsche, M., and Paulus, W. (2001). Sustained excitability elevations induced by transcranial DC motor cortex stimulation in humans. Neurology *57*, 1899 –1901.

S12. Monte-Silva, K., Kuo, M.F., Hessenthaler, S., Fresnoza, S., Liebetanz, D., Paulus, W., and Nitsche, M.A. (2013). Induction of late LTP-like plasticity in the human motor cortex by repeated non-invasive brain stimulation. Brain Stimulation *6*, 424-432.

S13. Poreisz, C., Boros, K., Antal, A., and Paulus, W. (2007). Safety aspects of transcranial direct current stimulation concerning healthy subjects and patients. Brain Research Bulletin *72*, 208–214.

S14. Gandiga, P., Hummel, F., and Cohen, L. (2006). Transcranial DC stimulation (tDCS): A tool for double-blind sham-controlled clinical studies in brain stimulation. Clinical Neurophysiology *117*, 845–850.

S15. Reinhart, R.M.G., and Woodman, G.F. (2015). Enhancing long-term memory with stimulation tunes visual attention in one trial. Proceedings of the National Academy of Sciences of the USA *112*, 625-630.

S16. Reinhart, R.M.G., Zhu, J., Park, S., and Woodman, G.F. (2015). Medial-frontal stimulation enhances learning in schizophrenia by restoring prediction-error signaling. Journal of Neuroscience *35*, 12232-12240.

S17. Reinhart, R.M.G., Zhu, J., Park, S., and Woodman, G.F. (2015). Synchronizing theta oscillations with direct-current stimulation strengthens adaptive control in the human brain. Proceedings of the National Academy of Sciences of the USA *112*, 9448-9453.

S18. Nunez, P.L., and Srinivasan, R. (2006). Electric fields of the brain: The neurophysics of EEG, 2nd Edition, (Oxford: Oxford University Press, Inc.).

S19. Woodman, G.F., and Luck, S.J. (2003). Serial deployment of attention during visual search. Journal of Experimental Psychology: Human Perception and Performance *29*, 121-138.

S20. Luck, S.J., and Hillyard, S.A. (1990). Electrophysiological evidence for parallel and serial processing during visual search. Perception & Psychophysics *48*, 603-617.

S21. Perrin, F., Pernier, J., Bertrand, O., and Echallier, J.F. (1989). Spherical splines for scalp potential and current density mapping. Electroencephalography and Clinical Neurophysiology *72*, 184-187.

S22. Polat, U., Ma-Naim, T., Belkin, M., and Sagi, D. (2004). Improving vision in adult amblyopia by perceptual learning. Proceedings of the National Academy of Sciences of the USA *101*, 6692–6697.

S23. Li, R.W., and Levi, D.M. (2004). Characterizing the mechanisms of improvement for position discrimination in adult amblyopia. Journal of Vision *4*, 476–487.

S24. Fronius, M., Chopovska, Y., Nolden, J., Loudon, S.E., Lüchtenberg, M., Zubcov, A., and Pepler, L. (2006). Occlusion treatment for amblyopia: assessing the performance of the electronic occlusion dose monitor. Strabismus *14*, 65-70.
S25. Levi, D.M., Polat, U., and Hu, Y.S. (1997). Improvement in Vernier acuity in adults with amblyopia. Practice makes better. Investigative Ophthalmology & Visual Science *38*, 1493–1510.
S26. Li, R.W., Young, K.G., Hoenig, P., and Levi, D.M. (2005). Perceptual learning improves visual performance in juvenile amblyopia. Investigative Ophthalmology & Visual Science *46*, 3161-3168.
S27. Li, R.W., Provost, A., and Levi, D.M. (2007). Extended perceptual learning results in substantial recovery of positional acuity and visual acuity in juvenile amblyopia. Investigative Ophthalmology & Visual Science *48*, 5046-5051.
S28. Zhou, Y., Huang, C., Xu, P., Tao, L., Qiu, Z., Li, X., and Lu, Z.L. (2006). Perceptual learning improves contrast sensitivity and visual acuity in adults with anisometropic amblyopia. Vision Research *46*, 739–750.
S29. Huang, C.B., Zhou, Y., and Lu, Z.L. (2008). Broad bandwidth of perceptual learning in the visual system of adults with anisometropic amblyopia. Proceedings of the National Academy of Sciences of the USA *105*, 4068-4073.
S30. Chen, P.L., Chen, J.T., Fu, J.J., Chien, K.H., and Lu, D.W. (2008). A pilot study of anisometropic amblyopia improved in adults and children by perceptual learning: An alternative treatment to patching. Ophthalmic and Physiological Optics *28*, 422–428.
S31. Levi, D.M., and Li, R.W. (2009). Perceptual learning as a potential treatment for amblyopia: a mini-review. Vision Research *49*, 2535-2549.
S32. Jennings, J.R., and Wood, C.C. (1976). The e-adjustment procedure for repeated-measures analyses of variance. Psychophysiology *13*, 277-278.
S33. Cohen, J. (1988). Statistical Power Analysis for the Behavioral Sciences, 2nd Edition, (New Jersey: Lawrence Erlbaum Associates).
S34. Antal, A., Nitsche, M.A., and Paulus, W. (2001). External modulation of visual perception in humans. Neuroreport *16*, 3553-3555.
S35. Accornero, N., Li Voti, P., La Riccia, M., and Gregori, B. (2007). Visual evoked potentials modulation during direct current cortical polarization. Experimental Brain Research *178*, 261–266.
S36. Antal, A., Varga, E.T., Kincses, T.Z., Nitsche, M.A., and Paulus, W. (2004). Oscillatory brain activity and transcranial direct current stimulation in humans. NeuroReport *15*, 1307-1310.
S37. Antal, A., Kincses, T., Nitsche, M., and Paulus, W. (2003). Manipulationof phosphene thresholds by transcranial direct current stimulation in man. Experimental Brain Research *150*, 375-378.
S38. Antal, A., Kincses, T.Z., Nitsche, M.A., and Paulus, W. (2003). Modulation of moving phosphene thresholds by transcranial direct current stimulation of V1 in humans. Neuropsychologia *41*, 1802-1807.
S39. Antal, A., Nitsche, M.A., Kruse, W., Kincses, T.Z., Hoffman, K.P., and Paulus, W. (2004). Direct current stimulation over V5 enhances visuo-motor coordination by improving motion perception in humans Journal of Cognitive Neuroscience *16*, 521-527.
S40. Mon-Williams, M., Tresilian, J.R., Strang, N.C., Kochhar, P., and Wann, J.P. (1998). Improving vision: neural compensation for optical defocus. Proceedings of the Royal Society B: Biological Sciences *265*, 71–77.
S41. Ohlendorf, A., and Schaeffel, F. (2009). Contrast adaptation induced by defocus – a possible error signal for emmetropization. Vision Research *49*, 249–256.
S42. Rajeev, N., and Metha, A. (2010). Enhanced contrast sensitivity confirms active compensation in blur adaptation. Investigative Ophthalmology & Visual Science *51*, 1242–1246.
S43. Mankowska, A., Aziz, K., Cufflin, M., Whitaker, D., and Mallen, E.A.H. (2012). Effect of blur adaptation on human parafoveal vision. Investigative Ophthalmology & Visual Science *53*, 1145–1150.
S44. Pesudovs, K., and Brennan, N.A. (1993). Decreased uncorrected vision after a period of distance fixation with spectacle wear. Optometry & Vision Science *70*, 528–531.
S45. George, S., and Rosenfield, M. (2004). Blur adaptation and myopia. Optometry & Vision Science *81*, 543–547.
S46. Yeshurun, Y., and Carrasco, M. (1998). Attention improves or impairs visual performance by enhancing spatial resolution. Nature *396*, 72-75.
S47. Anton-Erxleben, K., and Carrasco, M. (2013). Attentional enhancement of spatial resolution: linking behavioural and neurophysiological evidence. Nature Reviews Neuroscience *14*, 188-200.

S48. Mangun, G.R., and Hillyard, S.A. (1990). Allocation of visual attention to spatial location: Event-related brain potentials and detection performance. Perception and Psychophysics *47*, 532-550.
S49. Shiu, L., and Pashler, H. (1994). Negligible effect of spatial precuing on identification of single digits. Journal of Experimental Psychology: Human Perception and Performance *20*, 1037-1054.
S50. Shiu, L.P., and Pashler, H. (1995). Spatial attention and vernier acuity. Vision Res *35*, 337-343.
S51. Davson, H. (1990). Physiology of the eye, (London: The MacMillan Press Ltd).
S52. Jeffreys, D.A., and Axford, J.G. (1972). Source locations of pattern-specific components of human visual evoked potentials. II: Components of extrastriate cortical origin. Experimental Brain Research *16*, 22-40.
S53. Clark, V.P., Fan, S., and Hillyard, S.A. (1995). Identification of early visually evoked potential generators by retinotopic and topographic analyses. Human Brain Mapping *2*, 170-187.
S54. Di Russo, F., Martinez, A., and Hillyard, S.A. (2003). Source analysis of event-related cortical activity during visuo-spatial attention. Cerebral Cortex *13*, 486-499.
S55. Levi, D.M., and Polat, U. (1996). Neural plasticity in adults with amblyopia. Proceedings of the National Academy of Sciences of the USA *93*, 6830–6834.
S56. Li, R.W., Ngo, C., Nguyen, J., and Levi, D.M. (2011). Video-game play induces plasticity in the visual system of adults with amblyopia. Public LIbrary of Sciences Biology *9*, e1001135.
S57. Thompson, B., Mansouri, B., Koski, L., and Hess, R.F. (2008). Brain plasticity in the adult: modulation of function in amblyopia with rTMS. Current Biology *18*, 1067-1071.
S58. Spiegel, D.P., Byblow, W.D., Hess, R.F., and Thompson, B. (2013). Anodal transcranial direct current stimulation transiently improves contrast sensitivity and normalizes visual cortex activation in individuals with amblyopia. Neurorehabilitation and Neural Repair *27*, 760-769.
S59. Clavagnier, S., Thompson, B., and Hess, R.F. (2013). Long lasting effects of daily theta burst rTMS sessions in the human amblyopic cortex. Brain Stimulation *6*, 860-867.
S60. Camilleri, R., Pavan, A., Ghin, F., Battaglini, L., and Campana, G. (2014). Improvement of uncorrected visual acuity and contrast sensitivity with perceptual learning and transcranial random noise stimulation in individuals with mild myopia. Frontiers in Psychology *5*, 1234.
S61. Spiegel, D.P., Li, J., Hess, R.F., Byblow, W.D., Deng, D., Yu, M., and Thompson, B. (2013). Transcranial direct current stimulation enhances recovery of stereopsis in adults with amblyopia. Neurotherapeutics *10*, 831-839.
S62. Plow, E.B., Obretenova, S.N., Jackson, M.L., and Merabet, L.B. (2012). Temporal profile of functional visual rehabilitative outcomes modulated by transcranial direct current stimulation. Neuromodulation *15*, 367-373.
S63. Plow, E.B., Obretenova, S.N., Fregni, F., Pascual-Leone, A., and Merabet, L.B. (2012). Comparison of visual field training for hemianopia with active versus sham transcranial direct cortical stimulation. Neurorehabilitation and Neural Repair *26*, 616–626.